JOURNAL OF CATALYSIS **167,** 33–42 (1997)
ARTICLE NO. CA971590

A Theoretical Study of Butadiene Adsorption on the Pd–Ni Bimetallic System

P. Hermann, D. Simon,[1] P. Sautet, and B. Bigot

Laboratoire de Chimie Théorique,[2] Ecole Normale Supérieure de Lyon, 46 allée d'Italie, F-69364 Lyon, Cedex 07, France, and Institut de Recherches sur la Catalyse, 2 avenue Albert Einstein, F-69626 Villeurbanne, Cedex, France

Received November 15, 1995; revised November 28, 1996; accepted December 23, 1996

The calculated electronic perturbation of the butadiene molecule is identical when it is adsorbed either on the Pd–Ni bimetallic system or on the pure Pd surface. However, the calculations provide evidence that the butadiene adsorption strength is much smaller in the former case. The orbital by orbital analysis reveals that the π-d_{z^2} interaction is reduced, whereas the π^*-d_{yz} is enhanced with respect to the pure Pd surface. Nevertheless, since the total electron transfers from the π orbitals to the π^* orbitals within the butadiene molecule are similar, a two-electron analysis alone is unable to explain the large difference between the butadiene adsorption energy on the Pd–Ni surface alloy and that on pure Pd. This difference is partly related to anti-bonding interactions since the Pd–Ni bimetallic system exhibits a larger four-electron destabilization (roughly +25%). Evidence is also presented for a reduced electron exchange between the Pd–Pd adsorption site and its neighboring atoms in the case of the Pd–Ni bimetallic system with respect to the pure Pd and consequently a diminished coupling with the electron reservoir created by the extended surface. Hence, the adsorbing Pd clusters of a bimetallic system appear more isolated from the remaining part of the solid than they do in the pure Pd. © 1997 Academic Press

I. INTRODUCTION

The catalytic stability, selectivity, and/or activity of bimetallic systems are known to be superior in many cases to the analogous properties of a monometallic catalyst (1). Numerous theoretical and experimental studies, employing model catalysts, are aimed at the study of the changes that occur in the structural, electronic, and chemical properties of catalysts upon the addition of the second metal (2–10). A metal atom deposited on the surface of a second metal can exhibit large perturbations in its electronic and chemical properties. In many cases, the phenomena responsible for the perturbations have not been identified and the problem of understanding the properties of bimetallic systems is currently attracting new theoretical and experimental work.

The purpose of this paper is to focus on the Pd–Ni bimetallic system. The butadiene hydrogenation test reaction reveals that Pd atoms deposited on Ni(111) exhibit an activity similar to that of pure Pd (3, 4) for various Pd coverages (namely, from 0.5 to 3.0 monolayers). XPS studies show that the Pd $3d_{5/2}$ core level is shifted toward higher binding energies than those of the pure Pd surface atoms by at least 0.4 eV (4). In a previous paper (6), calculations based on an Extended-Hückel model, improved by the implementation of a two-body nuclear repulsion energy adapted from the correction technique used in the Anderson (ASED-MO) theory, have been performed on the naked Pd–Ni system. We have shown that the electronic structure of Pd atoms are altered compared to pure Pd, since a Pd(4d) electron depletion occurs. Moreover, a thermal treatment of the Pd deposits leads to an activity enhancement (roughly one order of magnitude) without any further electronic or selectivity alteration (3, 4). Geometrical modifications have consequently to be taken into account to explain the increased activity. Low energy ion scattering experiments have shown that the annealing leads to a Pd–Ni intermixing, giving rise to a surface alloy with a sharp Pd depth profile.

In this paper we examine the consequences of these phenomena on butadiene adsorption on the Pd–Ni bimetallic system as compared with the pure Pd surface, using an adapted ASED-MO method. Actually, this model alone cannot fully explain the reactivity toward butadiene hydrogenation. An improvement would be to check the behavior of butadiene adsorption in the presence of hydrogen. Nevertheless, if the role of hydrogen is considered as minor, as previously suggested (4), one can reasonably assume that the butadiene adsorption is a major step in the activity toward hydrogenation.

II. THE THEORETICAL METHOD

In our calculations, the butadiene is adsorbed on Pd atoms included in the first layer of a Ni(111) surface modeled by a semispherical-like cluster constituted by 114

---

[1] To whom correspondence should be addressed. E-mail: dsimon@chimie.ens-lyon.fr.

[2] This laboratory is part (UPR 5401) of the CNRS.

0021-9517/97 $25.00

TABLE 1

Extended Hückel Parameters

Atom	Orbital	H_{ii} (eV)	ζ_1	ζ_2	c_1	c_2
Ni	4s	−7.95	1.89			
	4p	−3.85	1.89			
	3d	−10.05	6.785	2.359	0.6462	0.5504
Pd	5s	−7.90	2.05			
	5p	−2.36	2.05			
	4d	−10.51	5.983	2.613	0.5535	0.6701
C	2s	−19.9	1.95		1	
	2p	−9.9	1.95		1	
H	1s	−12.1	1.35		1	

metallic atoms and exhibiting an extended surface. The large number of atoms involved in the calculations excludes the use of first principle methods. Periodic calculations are also not appropriated since the Pd–Ni surface alloy is not known as being ordered (3, 4).

This bimetallic surface has been studied in a previous work (6) within an adapted Extended-Hückel framework (11–13) including an electrostatic internuclear repulsion potential (6, 14–17). The main limitation of this semiempirical method is its non-self-consistent character. As a consequence, one of the drawbacks is the exaggerated electron charge drifts. Hence, atomic and molecular binding energy cannot be compared on a absolute scale. Nevertheless, its transparency and simplicity make it well suited for studying and analyzing chemical interactions on large systems by molecular orbital perturbation theory. The relative structural stabilities and qualitative *trends* in bonding are correctly described. The usefulness of bonding concepts, derived within the Extended-Hückel formalism in the case of extended systems with interfaces and adsorbed molecules has been convincingly demonstrated (18).

With an accurate choice of parameters, this all-valence-electron simplest semiempirical method provides a correct approximation to the electronic structure. The Hückel parameters used in our calculation (see Table 1) are chosen in order to reproduce experimental data: (i) the Fermi level difference between pure Ni and pure Pd is 0.2 eV (i.e., identical to the work function difference (19a)), (ii) the d-band of pure Pd is roughly 1.5 times wider than the Ni-band (19b), (iii) from X-ray diffraction experiments (20), the bulk interatomic distance of pure Pd and pure Ni are 2.74 and 2.49 Å, respectively, (iv) the optimum interatomic distances for the butadiene molecule in the gas phase are $d_{\mathrm{C=C}} = 1.34$ Å (21), $d_{\mathrm{C-C}} = 1.48$ Å (21), and $d_{\mathrm{C-H}} = 1.12$ Å (21). Compared to standard values, the H_{ii} values, which represent the energy of the atomic orbitals, are shifted upward for carbon and hydrogen, in order to simulate self-consistency and obtain a reasonable charge transfer between the surface and the adsorbed molecule (namely from 2 electrons to roughly 0.2).

The adsorption energy is expressed as

$$\varepsilon_{\mathrm{ads}} = \Delta E_{\mathrm{e^-}} + \Delta E_{\mathrm{rep}},$$

where $\Delta E_{\mathrm{e^-}}$ and ΔE_{rep} are calculated as a difference between the energy of a "cluster + adsorbed molecule" system and a "bare cluster with molecule in the gas phase" one. The orbital population calculations are based on a Mulliken analysis (22). Plotting the contribution of each orbital against the energy constitutes the local density of states (LDOS). A Gaussian broadening of the discrete spectrum obtained is applied in order to display the results of the calculations in terms of continuous density of states curves. For a single atom, the LDOS curve is obtained by cumulating all the atomic orbital LDOS.

III. BUTADIENE ADSORPTION

1. *General*

Experimental near edge X-ray adsorption fine structure (NEXAFS) studies (23) and another theoretical work (12) have already provided evidence for a di-π adsorption mode of the butadiene molecule on pure Pd(111). The di-π mode involves both butadiene double bonds (Fig. 1, left). Our theoretical results are also in favor of a butadiene di-π adsorption mode ($\varepsilon_{\mathrm{ads}} = -1.02$ eV) compared to the di-σ one (Fig. 1, right) involving only one of the double bonds of the molecule ($\varepsilon_{\mathrm{ads}} = -0.70$ eV). These results are consistent with experimental catalytic test data which indicate that the Pd(111) selectivity toward butenes is equal to unity. The adsorption energy of olefins (either π or di-σ adsorbed), being smaller than that of a di-π adsorption of the butadiene molecule, prevents butane formation as long as butadiene is present in the gas phase by removing butenes from the catalytic surface (24).

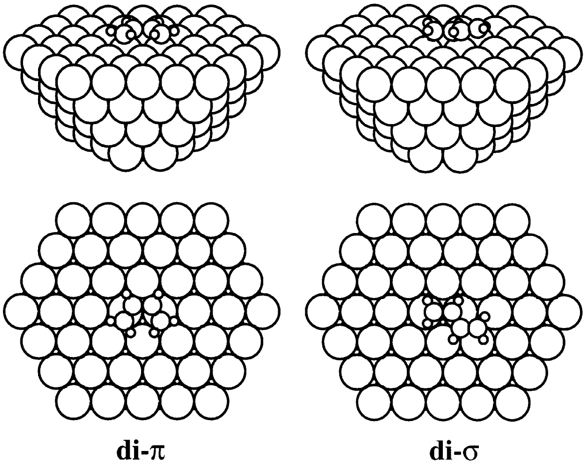

FIG. 1. Side and top views of di-π and di-σ coordination mode of butadiene on the 114 atom cluster.

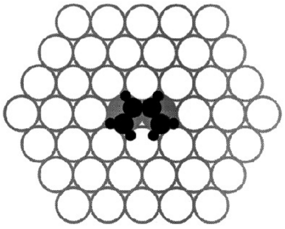

Pd_2 aggregate included in the first Ni(111) layer

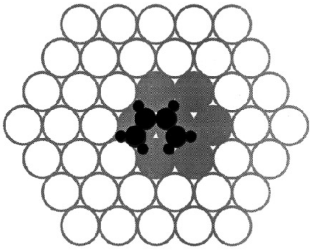

Pd_7 aggregate included in the first Ni(111) layer

FIG. 2. Di-π adsorption mode of the butadiene molecule on the Pd_2 aggregate included in the first Ni(111) layer and on the Pd_7 aggregate included in the first Ni(111) layer.

This particular adsorption geometry involves both butadiene double bonds and uses two contiguous metal atoms. In contrast with the pure Pd surface, the Pd–Ni bimetallic system exhibits three different types of adsorption site: the Pd–Pd site and the Pd–Ni and Ni–Ni ones. The assumption of a Pd homonuclear adsorption site is strongly supported by catalytic tests (5, 25), based on the decreasing number of Ni–Ni and Pd–Ni sites as the Pd coverage increases. Moreover, we have checked the different types of adsorption sites, and the calculations confirm the stability of the Pd–Pd site. Therefore, this paper is devoted to the study of the butadiene adsorption on the Pd–Pd active site of two sizes of Pd_n clusters (namely the Pd_2 and Pd_7 clusters) included in the first Ni(111) layer. Among various possible shapes for the Pd aggregates (see Fig. 2), the ones used for the study of the butadiene adsorption are the most stable within our theoretical model (6), the Pd atoms being all located in the same plane. Up to now, no experience allows one to obtain the atomic arrangement of the bimetallic surface. We have chosen to investigate the behavior of a small (Pd_2) and a large (Pd_7) cluster in the course of the butadiene adsorption. The electronic and geometrical properties of these surfaces have been studied in detail in a previous paper (6). We recall hereafter the most important results concerning the Pd–Ni surface alloy compared to the pure Pd.

Due to a charge transfer from Pd(4d) to the surrounding Ni atoms (0.13 e^-) and to a Pd(4d) → Pd(5s) electronic transfer, the Pd d-band is depleted by 0.17 e^-, whereas the s-band occupancy is slightly increased. Indeed, the alloying leads to a lower lying Pd d-band and to a destabilized Pd s-band. The computed Fermi level is $E_f = -9.60$ eV, i.e., 0.2 eV above the Fermi level of the pure Pd. The Pd LDOS, when they are projected on the orbitals mainly involved in the adsorption phenomena (d_{z^2} and d_{yz}), exhibit a poor density of states just below the Fermi level and a large contribution located at about −11.0 eV characteristic of the Pd–Ni interaction, illustrating a more localized character than in the pure Pd case. The Pd–Ni surface alloy also exhibits particular geometrical characteristics since the optimal computed Pd–Pd distances are found to be equal to 2.64 Å (for the Pd_2 cluster) and to 2.59 Å (for the Pd_7 cluster) instead of 2.74 Å for the pure Pd. The Pd–Ni distances are found to be 2.52 or 2.57 Å (Pd_2 case) and 2.54 Å (Pd_7 case). It has to be underscored that these distances between the adsorption site and its first neighbors are much shorter than in the pure Pd case.

Experimental studies (3, 4) have shown that the bimetallic surface selectivity toward butenes is equal to unity. This suggests that the butadiene adsorption mode on the bimetallic surface would also occur in a di-π mode. This statement is supported by our theoretical calculations. The computed adsorption energies on the Pd–Ni bimetallic system are displayed in Table 2 for both Pd_2 and Pd_7 clusters included in the first Ni layer. The difference between the di-π and the di-σ mode is similar to the case of pure Pd, supporting that the butadiene is expected to be di-π adsorbed on a Pd–Ni bimetallic surface.

Figure 2 depicts the adsorption sites in the case of the surface alloys. In the Pd_7 cluster case, among various adsorption sites, the most stable configuration (as a result of an optimization within our theoretical model) uses the central and the edge atoms of the Pd_7 aggregate. Due to the butadiene orientation on the surface, mainly the d_{z^2} and the d_{yz} metal orbitals are appropriated for an interaction with the butadiene frontier orbitals depicted in Fig. 3 (right). For symmetry reasons, only the π-d_{z^2} and the π^*-d_{yz} interactions will be considered in the qualitative study of the chemisorption. Actually, the π^* orbitals interact with both

TABLE 2

Comparison of the Butadiene Adsorption Energy for Pd_2 and Pd_7 Clusters Included in the First Ni(111) Layer

	Pd_2 in Ni		Pd_7 in Ni	
	di-σ	di-π	di-σ	di-π
ε_{ads} (eV)	−0.40	−0.62	−0.45	−0.65

Note. The optimized Hybridization parameters are $h = 0.5$ for the di-π geometry and $h = 0.65$ for the di-σ geometry.

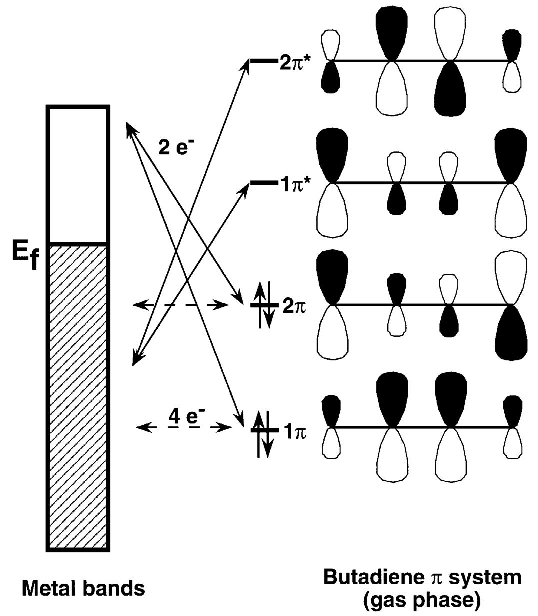

FIG. 3. Two- and four-electron interactions between the frontier orbitals of the butadiene and metal bands.

the d_{xz} and d_{yz} metal orbitals, since the C–C terminal bonds of the butadiene molecule are not parallel to the Pd–Pd site direction (x–z plane in Fig. 2). Nevertheless, the behavior of d_{xz} upon butadiene adsorption is analogous to that of d_{yz}, so we restrict the analysis of the π^* interaction to the d_{yz} metal orbital case.

Upon adsorption, the butadiene electronic structure is altered and this leads to geometrical distortions of the molecule. For the sake of simplicity, the geometrical distortions are assumed to be governed by a single parameter h (12), which measures the hybridization between the gas phase structure of butadiene (sp^2 hybridization) and the totally hybridized "sp^3 geometry" (corresponding to ethane). Whereas the C–H distances remain unchanged, the variations of C–C bond lengths, dihedral angles, and C–C–C angles between these two limiting cases are assumed to be linear with respect to the h parameter. In the case of the butadiene di-π adsorption mode on the bimetallic surface, the optimum h parameter is found to be equal to 0.5, suggesting that the butadiene is strongly altered upon adsorption. It has to be emphasized that this parameter is equal to the one calculated in the case of the pure Pd(111) surface (12). A detailed analysis of the butadiene electronic structure upon adsorption will be discussed in Section 2.

The metal–carbon distance is still under debate, since, to our knowledge, no particular work has been devoted to the butadiene adsorption on the Pd–Ni system surface. However, Ohtani *et al.* (26) have worked on benzene coadsorbed with carbon monoxide on Pd(111). Their theoretical treatment of the LEED data allows one to estimate the Pd–C distance. In the case of benzene, $d_{\mathrm{Pd-C}}$ is found to be 2.39 ± 0.05 Å, whereas 2.05 ± 0.05 Å is calculated for $d_{\mathrm{Pd-CO}}$. Other theoretical work (12) has assumed $d_{\mathrm{Pd-C}} = 2.1$ Å in the case of ethylene and butadiene adsorbed on Pd(111) on the basis of ethylene–Pd coordination complex experimental distances. This might suggest that the range 2.0 to 2.45 Å for the Pd–C distance is realistic. The optimal distance is found to be equal to 1.97 Å within our theoretical model. This indicates a tendency of the calculations to underestimate the Pd–C distance.

The interaction between the butadiene molecule and the bimetallic surface can be partitioned in three components: (i) the two-electron stabilizing interactions (between the π orbitals, or correspondingly the π^* orbitals, of the butadiene molecule and the vacant bands, or correspondingly the occupied bands, of the bimetallic system) visualized in Fig. 3, (ii) the four-electron destabilizing interactions (between occupied levels on both sides), (iii) the electrostatic nuclear interactions (between each of the atoms). The electronic factors are governed by the energetic position of the π and π^* orbitals with respect to the metal Fermi level and by their overlap with the surface metal bands. It has to be emphasized that the hybridization has an important influence on these electronic factors and consequently on the adsorption phenomena since increasing the h parameter leads to a destabilization of the π orbitals and to a stabilization of the π^* orbitals: they move closer to the Fermi level and consequently the two-electron interaction is enhanced. On the other side, the overlap of the π and π^* orbitals with the metal bands of the adsorption site decreases with increasing h, favoring the nonhybridized situation.

The four-electron interaction is, in a perturbation theory approach, proportional to the square of the overlap between the two interacting orbitals. One possible way of evaluating this interaction is to compute the following sum which is taken as a criterion for the four-electron destabilization strength:

$$I = \sum_{E_\mathrm{i}=E_\mathrm{b}}^{E_\mathrm{f}} S_{E_\mathrm{i}}^2. \qquad [1]$$

S_{E_i} stands for the overlap of all butadiene orbitals with the surface levels of energy E_i. E_b stands for the bottom energy of the metal bands and E_f for the metal Fermi level [12]. In order to improve this qualitative evaluation of the destabilization, one can take into account the electronic occupancy of the interacting orbitals since, upon adsorption, a part of some bands is expected to move above or below the Fermi level and cause an electron occupancy variation. Therefore the square of the overlap between the two interacting orbitals is corrected with their occupancy in order to give a weight "one" for plain four-electron interactions, a weight "zero" for two-electron interactions, and an intermediate weight for the other interaction.

In the course of the adsorption, the mainly involved metal bands widen. This phenomenon has also to be taken into account since the electron transfer is correlated with the band part which rises above or goes below the Fermi level and has an implication for the two- *and* the four-electron interactions.

The last interaction which has to be studied is the repulsive internuclear one, which we have implemented in the Extended Hückel framework, using an adapted ASED-MO model as explained above, and which we have already used in our previous work (6).

2. *Results and Analysis*

Table 3 displays the adsorption energy and Pd–C overlap populations in all the studied cases. The study of the computed adsorption energies reveals a large difference between the Pd–Ni bimetallic and the pure Pd surfaces ($\varepsilon_{\text{ads}} = -0.65$ and -0.62 eV for Pd_7 and Pd_2 clusters in the Ni(111) surface, respectively, and $\varepsilon_{\text{ads}} = -1.02$ eV for the pure Pd surface), indicative of a markedly diminished butadiene adsorption strength on the Pd–Ni system. Nevertheless, it appears that the Pd–C overlap populations are equal to 0.24 in all cases, suggesting that the metal–carbon bonds are similar on both the pure Pd and the bimetallic systems. This is not too surprising since the computed Pd–C distances are found to be equal on both kinds of surface, in contrast with the significant difference observed for the adsorption energies.

Table 4 describes the two-electron interactions and displays the π and π^* electron transfers, the total electron transfer, the butadiene π orbital mean electronic stabilization, defined as the difference between the mean electronic energy of the orbital after and before the adsorption. The mean electronic energy is calculated as the total energy of the electrons in this orbital, divided by the occupation of the orbital: hence it represents the mean energy per electron and is related to the stability of the orbital. For the π^* orbitals the mean electronic stabilization cannot be defined since they are empty before adsorption. The C=C overlap population, for the three types of surface, is also indicated in Table 4. In contrast with the qualitative rules generally invoked for the analysis of vibrational spectroscopy data (27), the butadiene electronic perturbations upon adsorption are similar on both the pure Pd and the Pd–Ni bimetallic systems. This is illustrated by the overlap population of the C=C bond, which is equal to 0.73 in all cases. It is not surprising since the optimal h parameter is equal to 0.5 in all cases and the π system total electron transfers are very similar (1.86 e^-, 1.87 e^-, 1.86 e^- for pure Pd and for Pd_7 and Pd_2 clusters, respectively). Nevertheless, the orbital by orbital analysis reveals some differences.

TABLE 3

Comparison of the Butadiene Adsorption Energy and Pd–C Overlap Population for Pure Pd, Pd_2, and Pd_7 Clusters Included in the First Ni Layer

	ε_{ads} (eV)	[Pd–carbon] overlap population
Pure Pd surface	−1.02	0.24
Pd_7 included in Ni(111)	−0.65	0.24
Pd_2 included in Ni(111)	−0.62	0.24

Note. The optimized hybridization parameter is $h = 0.5$ for the di-π geometry.

TABLE 4

Comparison of the C=C Overlap Population, Electron Transfer, and Mean Electronic Stabilization, Optimal for Butadiene Adsorbed on Pure Pd, Pd_2, and Pd_7 Clusters Included in the First Ni(111) Layer

	C=C overlap population	π and π^* interactions			
		Δp_π (e^-)	Δp_{π^*} (e^-)	$\lvert\Delta p_\pi\rvert + \Delta p_{\pi^*}$ (total π transfer)	ΔE_π (eV)
Pure Pd surface	0.73	−0.90	0.96	1.86	1π: −0.19 2π: −0.44
Pd_7 included in Ni(111)	0.73	−0.85	1.02	1.87	1π: −0.20 2π: −0.35
Pd_2 included in Ni(111)	0.73	−0.82	1.04	1.86	1π: −0.17 2π: −0.39
Butadiene gas	1.01	—	—	—	—

Note. The optimized hybridization parameter is $h = 0.5$ for the di-π geometry. The mean electronic stabilization is defined as the difference of the mean electronic energy after and before butadiene adsorption. Δp, electronic transfer upon adsorption; ΔE, mean energy stabilization upon adsorption.

The interactions of occupied π orbitals with the cluster molecular orbitals are weaker in the case of the Pd–Ni system since the associated electron transfer is smaller (−0.85 and −0.82 e^- for Pd_7 and Pd_2, respectively, compared with −0.90 e^- in the case of the pure Pd). Concomitantly, the 1π and 2π orbital energetic stabilization are weaker (see Table 4). This can be visualized by the LDOS projected on the π orbitals for the pure Pd and the Pd_2 cluster, depicted in Fig. 4. The part which rises above the Fermi level is greater for the pure Pd than for the bimetallic surface alloy. It can be understood in terms of (i) the Fermi level energetic location, which is lying 0.2 eV higher for the bimetallic system than for the pure Pd, and (ii) the Pd_2 cluster band, appearing more localized in energy and energetically lower-lying than the pure Pd one. Hence, the π interactions are likely to be reduced. Let us notice that the 1π orbital stabilization is less altered that the 2π one, since it is less interacting with the surface.

Table 5 displays the electron transfer and the stabilization of the d_{z^2} and d_{yz} orbital part of one of the Pd atoms in the adsorption site (defined as the difference of the mean electronic energy after and before adsorption, over all the occupied levels). The study of the d_{z^2} electron transfer reveals

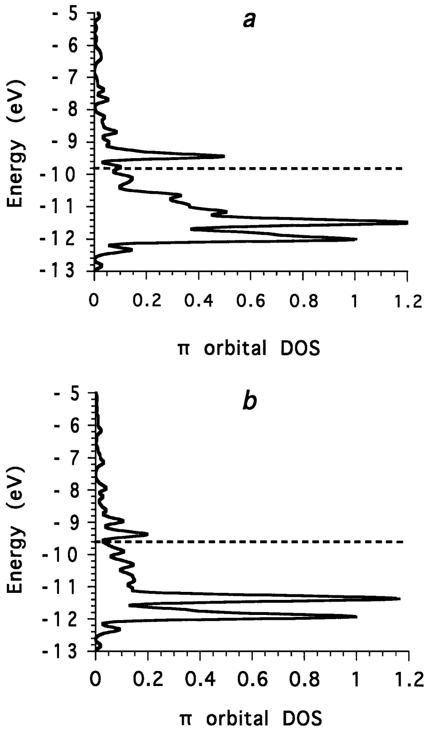

FIG. 4. Density of states projected on π orbitals of the butadiene molecule after adsorption. (a) Pure Pd case. (b) Pd_2 aggregate included in the first Ni(111) layer. The broken line indicates the Fermi level.

that the depletion is smaller in the case of the bimetallic system than in the pure Pd case (−0.62 for the pure Pd, −0.52 and −0.46 for Pd_7 and Pd_2, respectively). This occurs concomitantly and is consistent with the above-cited reduced π electron transfer. It is illustrated by the LDOS projected on the Pd d_{z^2} orbital, depicted in Fig. 5. The part of the band which rises above the Fermi level upon adsorption is smaller in the case of the Pd–Ni system (Figs. 5c and 5d) than in the pure Pd case (Figs. 5a and 5b). Let us note that the shape below the Fermi level remains roughly unchanged upon adsorption, in both the pure Pd case (Fig. 5b compared to Fig. 5a) and the Pd–Ni bimetallic system (Fig. 5d compared to Fig. 5c): in particular, the large contribution located at −11 eV is still present in the case of the alloy. The reduced d_{z^2}–π interaction can also be illustrated by the energetic stabilization of the d_{z^2} orbital upon adsorption (Table 5). As expected, it is smaller in the case of the bimetallic system with respect to the pure Pd surface (−0.32 and −0.27 eV for Pd_7 and Pd_2, respectively).

TABLE 5

Comparison of the Electron Transfer (Δp) and the Mean Electronic Stabilization (ΔE) for Butadiene Adsorbed on Pure Pd, Pd_2, and Pd_7 Clusters Included in the First Ni Layer

	d_{z^2}		d_{yz}	
	ΔP	ΔE (eV)	Δp	ΔE (eV)
Pure Pd surface	−0.62	−0.34	−0.38	−0.31
Pd_7 included in Ni(111)	−0.52	−0.32	−0.36	−0.32
Pd_2 included in Ni(111)	−0.46	−0.27	−0.36	−0.32

Note. The optimized hybridization parameter is $h = 0.5$ for the di-π geometry. The mean electronic stabilization is defined as the difference of the mean electronic energy after and before butadiene adsorption over all occupied levels.

The π^* interactions are enhanced (Table 4) since the associated electron transfers are greater (1.02 and 1.04 e^- for Pd_7 and Pd_2 respectively) than that seen in the pure Pd case (0.96 e^-). This can be illustrated by Fig. 6 which depicts the LDOS projected on the π^* orbitals. The part of the orbital which rises below the Fermi level is greater than in the case of the pure Pd, suggesting a better "π^*–surface" interaction in the case of the bimetallic system. This can be understood by considering the Fermi level energetic location of the Pd–Ni surface alloy which is calculated at −9.60 eV with respect to the pure Pd ($E_f = -9.80$ eV), i.e., 0.2 eV higher. Consequently the "π^*–surface" interaction is likely to be enhanced, suggesting that the Fermi level location prevails over the localized character of the *d* orbital.

Concerning the electron transfer of the d_{yz} orbital upon adsorption, the difference between the surface alloy and the pure Pd appears very slight since the d_{yz} orbital stabilization upon adsorption is nearly identical for both types of surface (Table 5). The part of the d_{yz} orbital which is expected to rise above the Fermi level upon adsorption (and therefore lead to an electron depletion) is smaller than the d_{z^2} one. The energetic location of the Fermi level (with respect to the pure Pd) allows a significant part of the d_{yz} band to remain below the Fermi edge. This can be illustrated by Fig. 7 which depicts the LDOS projected on the d_{yz} orbitals before and after adsorption (for the pure Pd and the Pd_2 cluster). If the Fermi level was located at −9.80 eV, as for the pure Pd, the electron depletion would be more important (namely −0.43). It has to be emphasized that the LDOS shape seems to be less altered upon adsorption (at least for the part of the band located below the Fermi level) with respect to the primitive shape (i.e., before adsorption) compared to the LDOS shape projected on the d_{z^2} orbital. This is explained by the fact that the d_{z^2} orbital interacts with the 1π and 2π orbitals, whose energies are close to the Pd d level, while d_{yz} interacts with vacant π^* orbitals located further away in energy.

Despite the fact that the surface geometry is kept frozen in our calculations, the surface morphology may change upon adsorption since the *d* orbitals of the Pd atoms of the adsorption site are electronically depleted. This may have an implication on the Pd–Pd bond. Figure 8 depicts the OPDOS (overlap population density of states) of the Pd–Pd adsorption site in the case of pure Pd. The lowest part of the *d* band is largely bonding before butadiene adsorption and the highest part is anti-bonding. The width of the

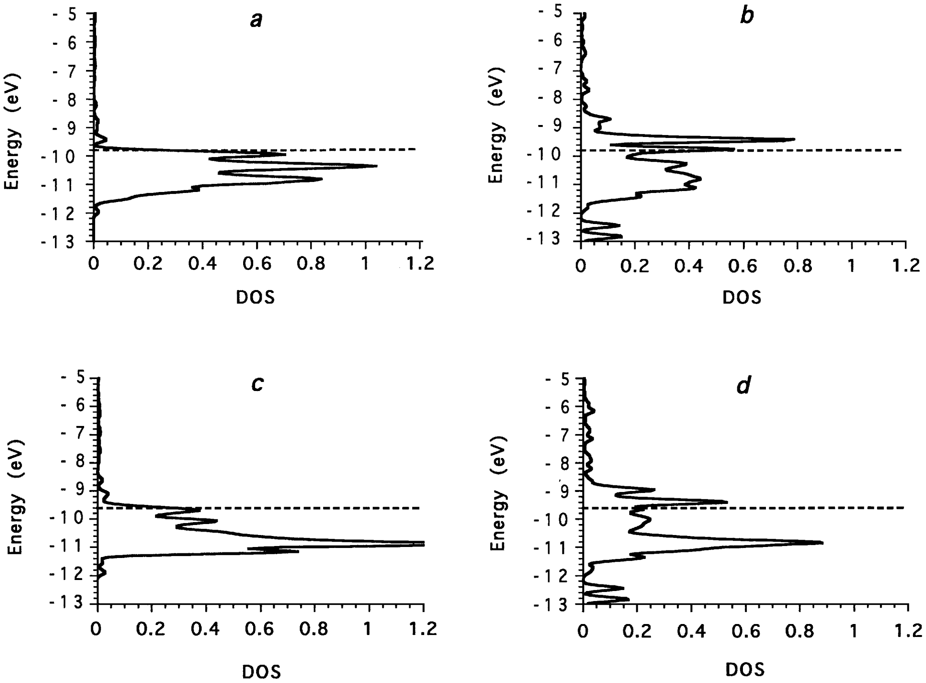

FIG. 5. Density of states projected on the d_{z^2} orbital of one Pd atom of the adsorption site. (a) Before adsorption on the pure Pd. (b) After adsorption on the pure Pd. (c) Before adsorption on the Pd$_2$ aggregate included in the first Ni(111) layer. (d) After adsorption on the Pd$_2$ aggregate included in the first Ni(111) layer. The broken line indicates the Fermi level.

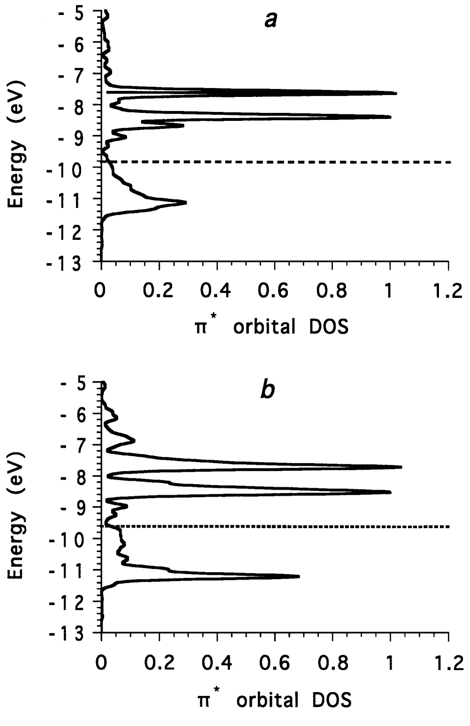

FIG. 6. Density of states projected on the π^* orbital of the butadiene molecule after adsorption. (a) Pure Pd case. (b) Pd$_2$ aggregate included in the first Ni(111) layer. The broken line indicates the Fermi level.

lower bonding part of the *d* orbitals suggests that it is rather delocalized. The shape of the OPDOS is essentially unchanged after adsorption except for the contribution located around −11.5 eV which becomes anti-bonding. The total overlap population of the Pd–Pd bond runs from 0.075 to 0.053 in the course of the adsorption, implying a slight adsorption-induced weakening of the Pd–Pd surface bond. Figure 9 depicts the OPDOS of the Pd–Pd bond of the bimetallic system. The *d* orbitals are more localized and mainly centered around −11 eV for the bonding part. The highest part of the band (anti-bonding) is broader than for the pure Pd case. Upon adsorption the OPDOS curve shows only a small decrease in the bonding area (Fig. 9). However, this is enough to yield a Pd–Pd overlap population decrease from 0.072 to 0.043, suggesting that the bond is more altered in the course of the adsorption than for the pure Pd case. This stronger perturbation of the bonds within the surface by the chemisorption in the case of the alloy is in good correspondence with the reduced binding energy, despite the similar Pd–C bond strength.

Table 6 displays the internuclear repulsion due to the butadiene approach and the four-electron interaction. The analysis of the internuclear repulsion reveals that the Pd–Ni surface exhibits a reduced repulsive interaction toward butadiene (1.12 and 1.06 eV for Pd$_7$ and Pd$_2$, respectively) compared with the pure Pd surface (1.16 eV). This is not surprising since numerous Ni atoms (smaller and exhibiting a smaller apparent charge than Pd) are part of the

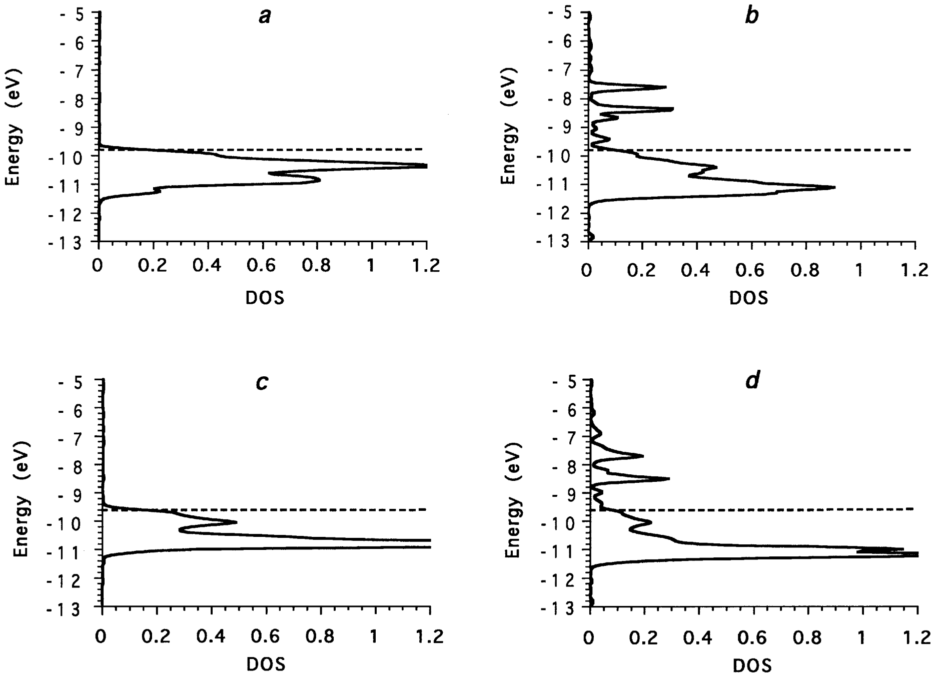

FIG. 7. Density of states projected on the d_{yz} orbital of one Pd atom of the adsorption site. (a) Before adsorption on the pure Pd. (b) After adsorption on the pure Pd. (c) Before adsorption on the Pd$_2$ aggregate included in the first Ni(111) layer. (d) After adsorption on the Pd$_2$ aggregate included in the first Ni(111) layer. The broken line indicates the Fermi level.

cluster. Nevertheless, the decreased nuclear repulsion energy seems not to be the relevant criterion to invoke, since its variation is small and in the opposite direction to the one expected for a destabilization of the butadiene molecule on the bimetallic surface. Therefore, the internuclear repulsion seems to be of secondary importance.

The study of the four-electron interaction reveals that the bimetallic system exhibits larger destabilizing interactions with respect to the pure Pd surface (0.20 for pure Pd, 0.25 and 0.24 in the Pd$_7$ and Pd$_2$ cases, respectively, i.e., +25 and +24% with respect to pure Pd). Whereas studies (in the case of pure Pd (28)) have shown that the Pd–Pd interatomic distance of the adsorption site has only a slight influence on the four-electron interaction, the adsorption site geometrical environment plays, on the contrary, a crucial role. Indeed, a large part of the four-electron destabilization comes from the interaction between C–H bond electrons and metal atom neighbors of the Pd–Pd adsorption site. Therefore, the interatomic distances between the adsorption site atoms and their first neighbors and the total electronic occupancy of these surrounding atoms seem to be of primary importance. For the Pd$_2$ and Pd$_7$ cluster case ($d_{\text{Pd–Ni}}$ are distributed around 2.54 Å), the atoms in the vicinity of the adsorption site are much closer to the molecule than in the case of pure Pd ($d_{\text{Pd–Pd}} = 2.74$ Å) and

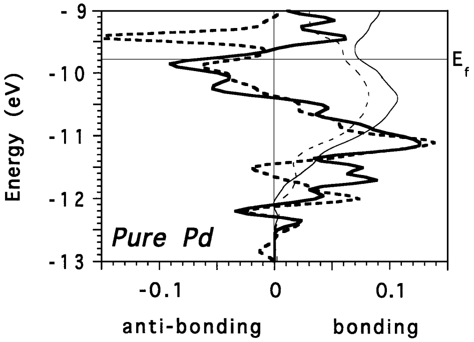

FIG. 8. Overlap population density of states of the Pd–Pd bond in the pure Pd case. Plain line, before adsorption, dashed line, after adsorption.

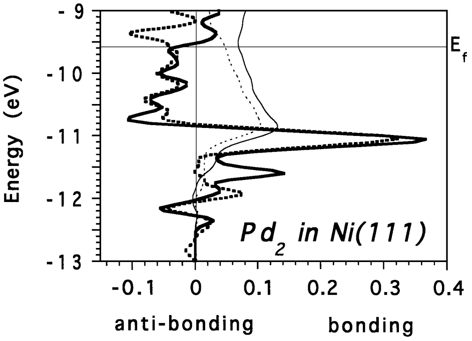

FIG. 9. Overlap population density of states of the Pd–Pd bond in the Pd$_2$ aggregate included in the first Ni(111) layer case. Plain line, before adsorption; dashed line, after adsorption.

these atoms exhibit a greater total electronic occupancy (namely around 10.2 e^-) than that seen in the pure Pd case (10.1 e^-). Even though these atoms are of different nature (namely Ni atoms, in the case of the Pd_2 cluster), exhibiting a narrower *d*-band than the Pd atoms, the four-electron interaction is increased compared with that of the pure Pd. Setting to zero the overlaps between the butadiene and the atoms which are not part of the adsorption site leads to reduced values of the [1] integral, to a stabilization of the butadiene molecule on the Pd–Ni bimetallic surface and to a diminished difference with respect to a pure Pd surface, indicating that a significant part of the four-electron destabilization comes from the butadiene interaction with atoms which are not part of the adsorption site. The four-electron interaction due to the adsorption site only (overlaps set to zero) are roughly similar.

3. *Discussion*

In the case of an adsorption on a metallic surface, the electron reservoir constituted by the metal plays an important role in the adsorption phenomena since all the electron transfers between a metal and an adsorbate are achieved through the adsorption site. The ability of the metallic surface to accept or give back electrons is crucial and governs part of the adsorption phenomena.

In the case of the butadiene adsorption, the metal acquires some electronic density from the π donation (which has to be distributed towards the reservoir through the adsorption site) and is able to backdonate some electron density towards the butadiene π^* system. Table 7 displays the electron transfer of the Pd–Pd adsorption site (which loses electrons) of the butadiene (which acquires electrons) and also the total electron transfer occurring in the course of the adsorption (sum of absolute values). The total electron transfer is smaller on the bimetallic surface, suggesting that the electron exchanges between the adsorption site and its neighborhood are less favored. It appears that electron depletion of the Pd–Pd site, in the case of the surface alloy, is smaller than for the pure Pd (−2.30 for the pure Pd, −2.16 and −2.00 for the Pd_7 and Pd_2, respectively). This is not surprising since these Pd atoms exhibit a smaller electron count (especially in *d* orbitals) before adsorption with respect to pure Pd surface atoms due to the alloying effect; therefore, they are less able to lose further electrons in the course of the adsorption. Nevertheless, it is on the bimetallic system that the electron transfer toward butadiene is the greatest. How can we explain this phenomenon?

The DOS projected on the *d* orbitals of the Pd atoms included in the first Ni layer exhibits, a particular shape since a strong contribution around −11.0 eV appears. In other words, the orbitals of the adsorption site are more localized in the bimetallic than on the pure Pd surface. Consequently, the electron exchange capability between the Pd and the Ni might be reduced. Hence the ability to distribute the electrons acquired through the π donation might be diminished. The backdonation is therefore favored toward the butadiene molecule. If we focus on the electron depletion of all the atom first neighbors of the adsorption site, upon adsorption, it is found to be 0.13 e^- per atom for the pure Pd and 0.09 e^- per atom for the bimetallic system. This diminished ability to lose electron charge may suggests that “adsorption site–reservoir” interactions are weakened with respect to the pure Pd. The following explanation is suggested. The heteroatomic Pd–Ni *d–d* interaction is weaker than the degenerate homoatomic Pd–Pd one. Hence, in the surface alloy, the Pd clusters are more isolated from the solid than they are in the pure Pd, with a less effective coupling with the reservoir. The alloy situation is then intermediate between the metal surface and the isolated cluster cases.

TABLE 6

Comparison of the Internuclear Repulsion Energy, Four-Electron Interaction, and Adsorption Energy for Butadiene Adsorbed on Pure Pd, Pd_2, and Pd_7 Clusters Included in the First Ni Layer

		Four-electron interaction		
	E_{rep} (eV)	All overlaps[a]	Overlaps set to 0[b]	E^b_{ads} (eV), Overlaps set to 0[b]
Pure Pd surface	1.16	0.20	0.14	−1.06
Pd_7 included in Ni(111)	1.12	0.25	0.16	−0.73
Pd_2 included in Ni(111)	1.06	0.24	0.15	−0.71

Note. The optimized hybridization parameter is $h = 0.5$ for the di-π geometry.

[a] All overlaps are taken into consideration.

[b] The overlaps between the butadiene molecule and metal atoms which are not part of the adsorption site are set equal to zero.

TABLE 7

Electron Transfer for the Butadiene Adsorption Site and the Butadiene Molecule

	Electron transfer for the Pd–Pd adsorption site	Electron transfer for the butadiene molecule	Total electron transfer
Pure Pd surface	−2.30	+0.06	+2.36
Pd_7 included in Ni(111)	−2.16	+0.17	+2.33
Pd_2 included in Ni(111)	−2.00	+0.22	+2.22

Note. The transfer is defined as the difference between the total electron occupancy after and before adsorption.

IV. CONCLUSIONS

The computed electronic perturbation of the butadiene molecule is identical when it is adsorbed either on the Pd–Ni bimetallic system or on the pure Pd surface. However, the calculations provide evidence that the butadiene adsorption strength is much smaller in the former case.

The π and π^* orbital analysis reveals that the $\pi \rightarrow d_{z^2}$ donation is reduced, whereas the $d_{yz} \rightarrow \pi^*$ retrodonation is enhanced. However, the depletion of d_{yz} is balanced by the occupation increase due to the Fermi level energy location, since the Pd–Ni surface alloy Fermi level is higher-lying (−9.60 eV) than the pure Pd one (−9.80 eV). In the same way, the interaction of the highest occupied contributions of d_{yz} with the butadiene π^* molecular orbital is enhanced. Nevertheless, the total amplitude of electron exchange between the butadiene and the metal being similar, the two-electron analysis is unable to explain, alone, the great difference between the butadiene adsorption energy on the Pd–Ni surface alloy and the pure Pd.

The study of destabilizing interactions allows a better understanding of the Pd–Ni system behavior. The Pd–Ni bimetallic system exhibits larger four-electron destabilizations (roughly +25%). The "adsorption-site-atoms to first-neighbour-atoms" distances are much shorter. Moreover, these latter atoms are more electron-rich than pure Pd surface atoms. Consequently, the four-electron interactions are likely to be increased toward adsorbates.

The electron exchanges between the adsorbate and the metallic surface are of primary importance in adsorption phenomena. Those exchanges are made via the adsorption site atoms. The bond type between the atoms of the adsorption site and the cluster ones which are not directly involved in adsorption phenomena might govern the efficiency of these exchanges. We have shown that, for this particular bond type, there is evidence for a reduced electron exchange in the case of the Pd–Ni bimetallic system with respect to the pure Pd, and hence coupling with the reservoir is weakened. Consequently, the Pd clusters appear more isolated from the solid than they do in the pure Pd. This could favor a diminished adsorption strength between the bimetallic system and the butadiene.

The hydrogen adsorption seems not to play a major role in the magnitude of the activity, since only a very slight difference in the isosteric heat of H_2 adsorption on pure Pd(111) (29) and on pure Ni(111) (30) is measured. This may also be the case on the Pd–Ni bimetallic system (4). Therefore, assuming that the butadiene adsorption is the reaction rate-determining step, the reduced adsorption strengths might lead to a greater hydrogenation turnover. This would be consistent with experimental data which indicate that the butadiene hydrogenation turnover is larger on the bimetallic system than on pure Pd (3, 4).

Nevertheless, the possible coadsorption of butadiene and hydrogen has not been elucidated by our model. In particular, in such conditions the presence of hydrogen adsorption could modify the role of surrounding Ni. It would be useful to study the Ni–Pd and Ni–Ni sites close to hydrogen adsorption sites in order to assess whether Ni acts only as an electron reservoir or provides modified adsorption sites. Calculations on this are now in progress.

ACKNOWLEDGMENTS

We are grateful to the Institut du Développment et des Ressources en Informatique Scientifique (IDRIS) of the Centre National de la Recherche Scientifique (CNRS France) for generous allocation of computer time.

REFERENCES

1. Sinfelt, J. H., "Bimetallic Catalysts." Wiley, New York, 1983.
2. Miegge, P., Rousset, J. L., Tardy, B., Massardier, J., and Bertolini, J.-C., *J. Catal.* **149**, 404 (1994).
3. Hermann, P., Tardy, B., Simon, D., Guigner, J.-M., Bigot, B., and Bertolini, J.-C., *Surf. Sci.* **307/309**, 422 (1994).
4. Bertolini, J.-C., Miegge, P., Hermann, P., Rousset, J.-L., and Tardy, B., *Surf. Sci.* **331/333**, 651 (1995).
5. Hermann, P., Tardy, P., Jugnet, Y., Simon, D., and Bertolini, J.-C., *Catal. Lett.* **36**, 9 (1996).
6. Hermann, P., Simon, D., and Bigot, B., *Surf. Sci.* **350**, 301 (1996).
7. Rodriguez, J. A., *Surf. Sci.* **318**, 253 (1994) and references therein.
8. Rodriguez, J. A., and Kuhn, M., *J. Phys. Chem.* **98**, 11251 (1994).
9. Ruckmann, M. W., and Strongin, M., *Acc. Chem. Res.* **27**, 250 (1994).
10. Castellani, N. J., and Légaré, P., *J. Phys. Chem.* **98**, 9606 (1994).
11. Hoffmann, R., *J. Chem. Phys.* **39**, 1397 (1963).
12. Sautet, P., and Paul, J. F., *Catal. Lett.* **9**, 245 (1991).
13. Delbecq, F., and Sautet, P., *Langmuir* **9**, 245 (1993).
14. Anderson, A. B. J., *J. Chem. Phys.* **60**, 2477 (1974).
15. Anderson, A. B. J., and Hoffmann, R., *J. Chem. Phys.* **60**, 4271 (1974).
16. Calzaferri, G., Forss, L., and Kamber, I., *J. Chem. Phys.* **93**, 5366 (1989) and references therein.
17. Savary, F., Weber, J., and Calzaferri, G., *J. Chem. Phys.* **97**, 3722 (1993).
18. Hoffmann, R., "Solids and Surfaces: A Chemist's View of Bonding in Extended Structures." VCH, Weinheim, 1988.
19. (a) Michaelson, H., B., *J. Appl. Phys.* **48**, 4729 (1977); (b) Nordlander, P., Holloway, S., and Nørskov, J. K., *Surf. Sci.* **136**, 59 (1985).
20. Greenwood, N. N., and Earnshaw, A., "Chemistry of the Elements." Pergamon, Oxford, 1994.
21. March, J., "Advanced Organic Chemistry" McGraw-Hill, Kogakusha Ltd., New York, 1986.
22. Mulliken, R. S., *J. Chem. Phys.* **23**, 1833 (1955).
23. Bertolini, J.-C., Cassuto, A., Jugnet, Y., Massardier, J., Tardy, B., and Tourillon, G., *Surf. Sci.* **349**, 88 (1996).
24. Ouchaib, T., Massardier, J., and Renouprez, A., *J. Catal.* **119**, 517 (1989).
25. Hermann, P., Guigner, J.-M., Tardy, B., Jugnet, Y., Simon, D., and Bertolini, J.-C., *J. Catal.* **163**, 169 (1996).
26. Ohtani, H., van Hove, M. A., and Somorjai, G. A., *J. Phys. Chem.* **92**, 3974 (1988).
27. Gates, J. A., and Kesmodel, L. L., *Surf. Sci.* **120**, L461 (1982).
28. Hermann, P., thesis, Lyon, 1996.
29. Conrad, H., Ertl, G., Koch, J., and Latta, E. E., *Surf. Sci.* **41**, 435 (1974).
30. Christmann, K., Schober, O., Ertl, G., and Neumann, M. J., *J. Chem. Phys.* **60**, 4528 (1973).